arXiv:1404.2449v1 [cond-mat.supr-con] 9 Apr 2014

Nodal Landau Fermi-Liquid Quasiparticles in Overdoped $La_{1.77}Sr_{0.23}CuO_4$

C. G. Fatuzzo,[1] Y. Sassa,[2] M. Månsson,[2,3] S. Pailhès,[4,5] O. J. Lipscombe,[6] S. M. Hayden,[6]
L. Patthey,[7] M. Shi,[7] M. Grioni,[1] H. M. Rønnow,[1] J. Mesot,[1,2,4] O. Tjernberg,[3] and J. Chang[1,7,4]

[1]*Institute for Condensed Matter Physics, École Polytechnique Fedérale de Lausanne (EPFL), CH-1015 Lausanne, Switzerland*
[2]*Laboratory for Solid State Physics, ETH Zürich, CH-8093 Zürich, Switzerland*
[3]*KTH Royal Institute of Technology, Materials Physics, S-164 40 Kista, Sweden*
[4]*Laboratory for Neutron Scattering, Paul Scherrer Institut, CH-5232 Villigen, Switzerland*
[5]*LPMCN, CNRS, UMR 5586, Université Lyon 1, F-69622 Villeurbanne, France*
[6]*H. H. Wills Physics Laboratory, University of Bristol, Bristol, BS8 1TL, United Kingdom*
[7]*Swiss Light Source, Paul Scherrer Institut, CH-5232 Villigen PSI, Switzerland*

Nodal angle resolved photoemission spectra taken on overdoped $La_{1.77}Sr_{0.23}CuO_4$ are presented and analyzed. It is proven that the low-energy excitations are true Landau Fermi-liquid quasiparticles. We show that momentum and energy distribution curves can be analyzed self-consistently without quantitative knowledge of the bare band dispersion. Finally, by imposing Kramers-Kronig consistency on the self-energy Σ, insight into the quasiparticle residue is gained. We conclude by comparing our results to quasiparticle properties extracted from thermodynamic, magneto-resistance, and high-field quantum oscillation experiments on overdoped $Tl_2Ba_2CuO_{6+\delta}$.

I. INTRODUCTION

The extent to which Landau Fermi-liquid theory, and its concept of quasiparticles[1], applies to the normal state of cuprates is still under debate[2,3]. Evidence for Landau Fermi-liquid quasiparticles has been reported by resistivity experiments on highly overdoped $La_{2-x}Sr_xCuO_4$ (LSCO)[4]. More recently, unambiguous proof has been given by high-field quantum oscillation experiments[5–9] on both overdoped and underdoped cuprates. It is, however, puzzling that no evidence of Landau Fermi-liquid quasiparticle excitations has been found from angle resolved photoemission spectroscopy (ARPES), that is a direct probe of the Green's function: $-(1/\pi)\mathrm{Im}G(k,\omega)$[10]. Although the "quasiparticles" terminology is widely used to describe the excitations of the photoemission spectra, it has never been proven by ARPES that the low-energy excitations in the cuprates are indeed true Landau Fermi-liquid quasiparticles. A direct spectroscopic proof of true Landau Fermi-liquid quasiparticles in the cuprates is therefore important.

This paper has two main objectives. The first is to prove that the nodal excitations observed in overdoped LSCO by ARPES are genuine Landau Fermi-liquid quasiparticles. The second is to discuss the nodal bare band velocity, v_b, and the nodal quasiparticle residue $Z \equiv (1 - \partial\Sigma'/\partial\omega)^{-1}$, where Σ is the self-energy. Perhaps the most compelling spectroscopic proof of Landau quasiparticles is the demonstration of a low-energy self-energy that has (1) the form $\Sigma'' \propto i\omega^2$[11] and (2) $-Z\Sigma'' < |\omega|$[12,13]. Proving this requires full knowledge about Σ and insight into the bare band ε_b, that is not straightforward to derive from an APRES spectrum[14]. Here, we however present an experimental case where $Z\Sigma''$ can be evaluated without quantitative knowledge of ε_b. In this specific case, it is therefore possible to prove the existence of true Landau Fermi-liquid quasiparticle excitations.

II. METHODS

Nodal ARPES spectra of overdoped $La_{1.77}Sr_{0.23}CuO_4$ ($T_c = 25$K)[22,23] were recorded at the surface and interface spectroscopy (SIS) beam line[19] of the Swiss Light Source (SLS) at the Paul Scherrer Institute, Switzerland. High quality nodal spectra were obtained after cleaving[21] at $T = 15$ K under ultra-high vacuum conditions ($p \sim 10^{-11}$ mbar). Using 55 eV circular polarized photons and a SCIENTA 2002 electron analyzer, angular and energy resolutions corresponding to 0.15° (FWHM) and $\sigma = 9$ meV (standard Gaussian deviation) were achieved. A detailed description of the experimental conditions can be found in Ref. 20.

III. RESULTS

Fig. 1(a) shows a colormap – I vs (k,ω) – of ARPES spectra recorded close to the nodal direction of overdoped $La_{1.77}Sr_{0.23}CuO_4$. A selection of corresponding momentum distribution curves (MDC) and energy distribution curves (EDC) are displayed in Fig. 1(b,c). We start by discussing the MDCs. As this paper focuses entirely on the low-energy excitations, MDCs are only shown up to the energy scale (80 meV) of the nodal kink shown in the inset of Fig. 1(c). In this energy interval, the MDC line shapes are symmetric peaks on a constant background. Therefore, data at constant ω were analyzed using a Lorentzian function $I_0\Gamma/[(\omega - \varepsilon_k)^2 + \Gamma^2]$, where Γ is the linewidth (Fig. 2a), ε_k is the peak position (Fig. 2b), and I_0 is an amplitude (Fig. 3). The observed nodal excitations disperse with a Fermi velocity $v_F = 1.62(2)$ eVÅ [Fig. 2(b)], consistently with previous reports on LSCO[24,25]. The half-width half-maximum, Γ, is plotted as a function of excitation energy squared ω^2 in Fig. 2(a). We find that, for $\omega < \omega_c = 0.18 \pm 0.2$ eV, the linewidth is well described by $\Gamma = \Gamma(0) + \eta\omega^2$ with

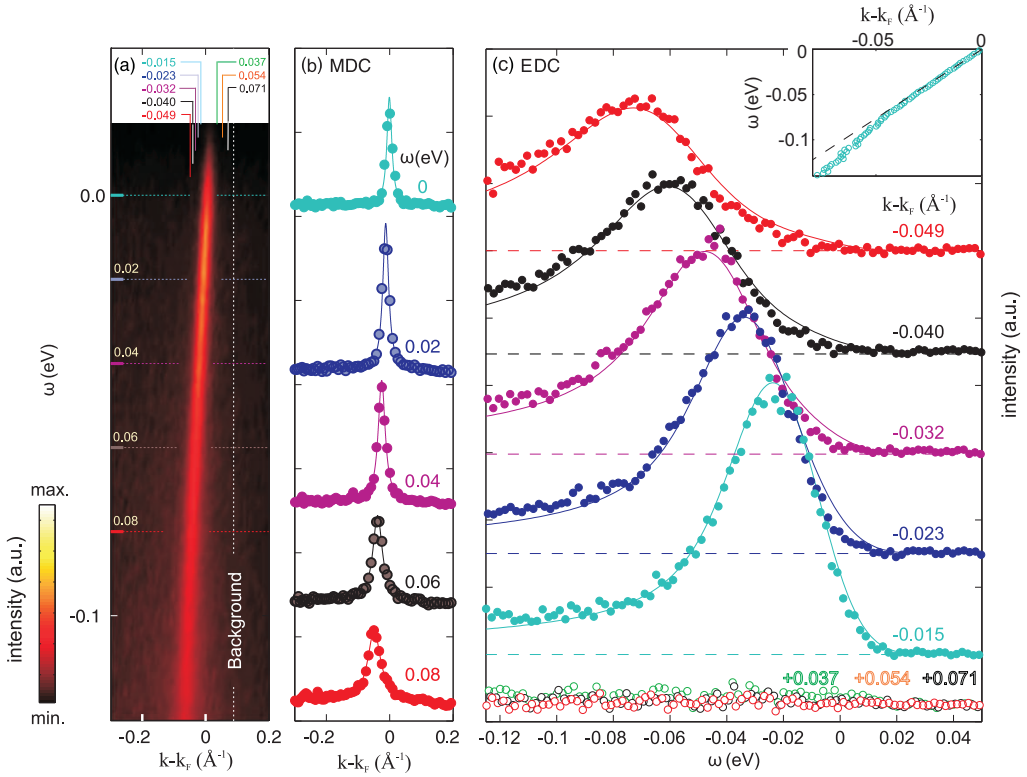

FIG. 1: (a) Nodal ARPES spectra recorded from overdoped LSCO ($x = 0.23$), at $T = 15$ K with 55 eV photon. The intensity, displayed versus momentum $k - k_F$ (horizontal) and excitation energy ω (vertical), has a false color scale with white as the most intense as indicated by the colorbar. (b) Momentum distribution curves (MDCs) of the spectra shown in (a), for fixed energies as indicated. Solid lines are Lorentzian fits to the data. (c) Energy distribution curves (EDCs) recorded at momenta as indicated. A ω-dependent background defined by the EDC at $k - k_F = 0.089$ Å^{-1} (indicated by the vertical white dashed line in (a)) has been subtracted. Solid lines display the ω-dependence of Eq. 3, multiplied with the Fermi-Dirac distribution and convoluted with the instrumental resolution[18]. For the sake of visibility, data in (b) and (c) are arbitrarily shifted in the vertical direction. The insert of (c) displays the excitation dispersion derived from MDC analysis of the spectra in (a).

$\eta = 3.14(4)$ eV^{-2}Å^{-1}, and $\Gamma(0) = 0.0117(1)$ Å^{-1}. The elastic scattering $\Gamma(0)$ is lower than what is usually reported for LSCO[25,26]. As impurity scattering is one source of elastic scattering[27], low values of $\Gamma(0)$ may be an indication of high sample quality.

To reveal the intrinsic physical line shape, a background has been subtracted from the EDCs shown in Fig. 1(c). The energy dependent background was extracted from the spectra using an energy distribution curve on the un-occupied side of the dispersion (indicated by a vertical dashed line in Fig. 1(a)). This is a common procedure[28] and an example of a raw background spectrum can be found in the supplement of Ref. 20. In this fashion, EDCs recorded at a momentum $|k|$ larger than the Fermi momentum $|k_F|$ [displayed with open circles in Fig. 1(c)] are featureless, demonstrating the successful background subtraction. On the other hand, EDCs with $k < k_F$ [full circles] reveal the intrinsic line shape of the excitations.

IV. DISCUSSION

The measured ARPES intensities $I(k,\omega)$ can be modelled by a product of the spectral function $A(k,\omega) = -(1/\pi)\mathrm{Im}G(k,\omega)$, a matrix element $M(k,\omega)$, and the Fermi distribution $f(\omega)$[10]. Matrix elements typically vary weakly as a function of (k,ω). Notice that the excitations shown in Fig. 1(b) disperse over less than 10 percent of the Brillouin zone. It is therefore not unreasonable to ignore matrix element effects. In that case, the ARPES intensity becomes a direct measure of the occupied part of the spectral function. It is common practice to separate the spectral function into coherent and incoherent parts, *i.e.* $A(k,\omega) = A_{coh}(k,\omega) + A_{inc}(k,\omega)$[10]. The coherent part can be written as:

$$A_{coh}(k,\omega) = \frac{-1}{\pi}\frac{\Sigma''(k,\omega)}{(\omega - \Sigma'(k,\omega) - \varepsilon_b)^2 + \Sigma''(k,\omega)^2} \quad (1)$$

where ε_b is the *a priori* unknown bare band, and the self-energy must obey $|\Sigma'| \gg |\Sigma''|$[31]. Experimentally, one would associate sharp dispersing features to the coherent

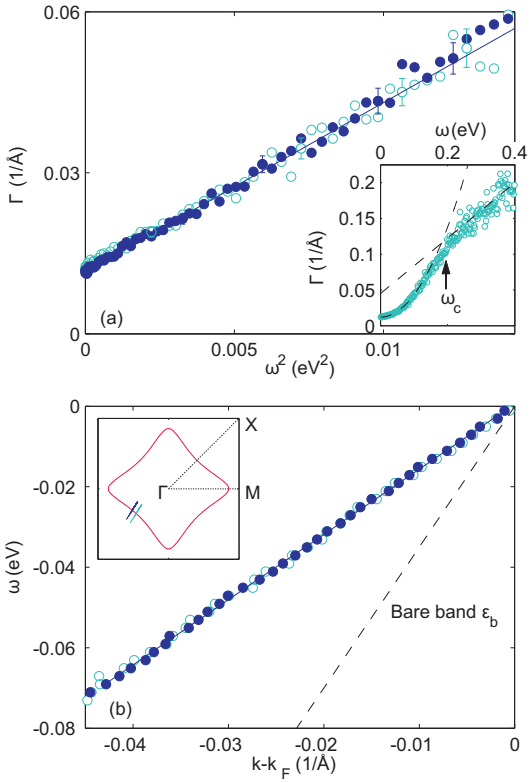

FIG. 2: (a) Linewidth Γ of the momentum distribution curves plotted versus excitation energies squared (ω^2), for the two cuts shown in the inset of (b). Inset of (a) shows Γ vs ω. The deviation from ω^2 dependence defines the energy scale ω_c[20] – indicated by the arrow. (b) Nodal dispersions extracted from MDC analysis for the two cuts shown in the inset. The dashed line indicates the bare-band extracted by assuming Kramers-Kronig consistency of the self-energy Σ, see text. The inset shows the Fermi surface of LSCO $x = 0.23$ and the two cuts along which the spectra were recorded.

part of the spectral function and featureless weight to the incoherent part. Here we focus on the low-energy part of the spectra, where the coherent spectral weight is dominating.

To make progress, two justified assumptions are made. First, it is assumed that the experimentally unknown bare band can be linearized ($\varepsilon_b \simeq v_b(k - k_F)$) near the Fermi level. Already the observed normalized band (extracted from the MDC analysis) can, to a very good approximation, be described by $\varepsilon_k = v_F(k - k_F)$, with $v_F = 1.62$ eVÅ [Fig. 2(b)]. The bare band is expected to have an even larger band velocity – LDA calculations suggest for example $v_b \simeq 3.5$ eVÅ[29]. For the excitation energies discussed here, curvature effects of the bare band are therefore expected to be negligibly small. Secondly, we assume that the self-energy, Σ, is locally momentum independent. Globally this assumption is not correct – the self-energy varies strongly as one approaches the anti-nodal region[20]. However, locally, in the vicinity of the nodal region, this is a good approximation. As shown in Fig. 2, both the band velocity and MDC linewidth are essentially identical for the two different nodal cuts. Another indication that Σ is momentum independent stems from the symmetric MDC lineshape shown in Fig. 1b. A k-dependence of Σ along the cut-direction would lead to an asymmetric lineshape. As this is not observed, it is concluded that Σ is locally independent of momentum both along and perpendicular to the cut direction.

It is thus possible to rewrite the coherent part of the spectral function as:

$$A_{coh}(k,\omega) = \frac{-1}{\pi}\frac{\Sigma''(\omega)}{(\omega - \Sigma'(\omega) - v_b(k - k_F))^2 + \Sigma''(\omega)^2}. \quad (2)$$

Notice that this is nothing else than a Lorentzian function in momentum space, with half-width half-maximum Γ given by $\Gamma(\omega) = -\Sigma''(\omega)/v_b$. Experimentally, it is found that $\Gamma \propto \omega^2$ (see Fig. 2). Therefore, consistently with true Fermi liquid quasiparticle excitations, we conclude that $\Sigma'' \propto \omega^2$.

A Kramers-Kronig consistent self-energy with $\Sigma'' \propto \omega^2$ has $\Sigma' \simeq -\gamma\omega$ in the low-energy limit. The unknown constant γ is sometimes referred to as the quasiparticle renormalization factor[30]. If consistency between MDC and EDC poles (dispersions) is enforced, then $1/(1+\gamma) = v_F/v_b = Z$. The coherent spectral function can consequently be re-written as:

$$A_{coh}(k,\omega) = \frac{Z}{\pi}\frac{v_F\Gamma}{(\omega - v_F(k - k_F))^2 + (v_F\Gamma)^2}, \quad (3)$$

where both v_F and Γ are known from the MDC analysis. The only unknown parameter, v_b, is a prefactor. It is therefore possible to model the EDC lineshape without quantitative knowledge of the bare band ϵ_b, and with the peak amplitude as the only free parameter – see solid lines in Fig. 1(c). In the displayed energy interval, a consistent description of both EDCs and MDCs were obtained from $A_{coh}(k,\omega)$.

Because $Z = v_F/v_b$ and $\Sigma'' = -\eta v_b\omega^2$, the product $Z\Sigma'' = -v_F\eta\omega^2$ can be evaluated without quantitative knowledge of the bare band velocity. The condition for coherent quasiparticle excitations is $-Z\Sigma'' < |\omega|$[12,13]. Using the experimental values of v_F and η, we find that Landau quasiparticles are coherent for $\omega < 1/v_F\eta \sim 0.19$ eV. This energy scale is comparable to ω_c – the energy scale below which $\Sigma'' \propto \omega^2$ – and hence re-enforces the interpretation of ω_c as an energy scale related to the break down of Landau Fermi-liquid quasiparticle excitations[20].

Finally, we discuss the Kramers-Kronig relation between Σ′ and Σ″:

$$\Sigma' = \frac{\mathcal{P}}{\pi}\int_{-\omega_c}^{\omega_c}\frac{\Sigma''(\omega')}{\omega' - \omega}d\omega' \pm \frac{\mathcal{P}}{\pi}\int_{\pm\omega_c}^{\pm W}\frac{\Sigma''(\omega')}{\omega' - \omega}d\omega' \quad (4)$$
$$= \Sigma'_{qp} + \Sigma'_{nqp}$$

where $\mathcal{P}$ is the principal value and W is the band width. To first order, the quasiparticle part yields $\Sigma'_{qp} \simeq \gamma_{qp}\omega$

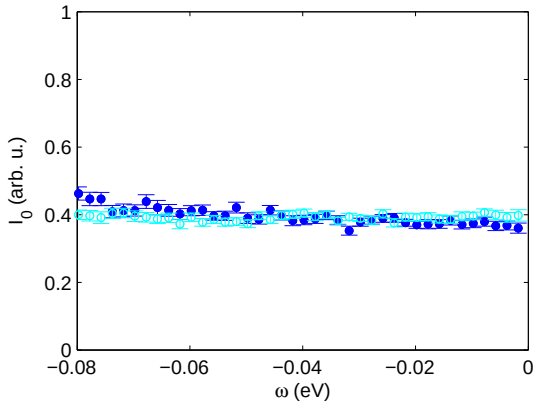

FIG. 3: Amplitude I_0, in arbitrary units, versus excitation energy ω fot the two cuts in the inset of Fig. 2b. Correction by the Fermi-Dirac distribution only influence the data points near the Fermi level.

where $\gamma_{qp} = 2v_b\eta\omega_c/\pi$. To gain insight into Σ'_{nqp}, we define $Z_i(\omega) = (1 - \partial \mathrm{Re}\Sigma_i/\partial\omega)^{-1}$ so that $Z(\omega) = Z_{qp}(\omega) + Z_{nqp}(\omega)$. As $Z(\omega) \sim I_0(\omega)$ varies weakly with excitation energies (see Fig. 3), we infer that Z_{nqp} (to first order) is ω-independent . Hence $\mathrm{Re}\Sigma_{nqp}(\omega) = \gamma_{nqp}\omega$ and $Z = 1/(1+\gamma_{qp}+\gamma_{nqp})$. As long as the detailed high-energy part of $\mathrm{Im}\Sigma(\omega)$ is unknown, it is not possible to directly extract $\Sigma'_{nqp} = \gamma_{nqp}\omega$. This is known as the "tail" problem[14]. The linear ω-dependence at high-energies, shown in the inset of Fig. 2, yields $\gamma_{nqp} \sim \ln(C/\omega_c)$ where C is an unknown constant. Hence γ_{nqp} diverges only logaritmically in the limit $\omega_c \to 0$[20]. On the other hand, for large ω_c the role of γ_{nqp} will be less important. As $\omega_c = 0.18$ eV is a large energy scale, corresponding to a temperature scale of the order 1000 K, we hypothesize that $\gamma_{nqp} \ll 1$. In that case, $Z \simeq 1/(1+\gamma_{qp}) = v_F/v_b$ and hence $v_b = \pi v_F/(\pi - 2\eta\omega_c v_F) = 3.8$ Å. This is consistent with the nodal LDA Fermi velocity $v_{LDA} = 3.5$ eVÅ[29] calculated for LSCO and with values of v_b derived from a numeric self-consistent method[14]. The consistent values of v_b further support the conjecture that $\gamma_{nqp} \ll 1$.

The quasiparticle mass is given by $m_b/m^* = Z\hat{Z}$, where m_b is the bare mass and $\hat{Z} = 1 + (m_b/\hbar^2 k_F)\partial\Sigma'(k,0)/\partial k$[17,31]. Since the self-energy is locally independent of momentum, the nodal quasiparticle mass is given by $m^* = m_b/Z \simeq 2.4m_b$. This is comparable to the momentum averaged values $m^* \simeq 3m_b$ extracted from quantum oscillation[6,17] and electronic specific heat experiments on overdoped $Tl_2Ba_2CuO_{6+\delta}$ (Tl2201)[15]. Remarkably, a Fermi-liquid cut-off energy scale $\omega_c \sim 0.2$ eV was extracted[32,33] from angle-dependent magneto-resistance measurements on overdoped Tl2201[16]. This is in good agreement with nodal ARPES spectra recorded on LSCO $x = 0.23$[20]. On LSCO, no quantum oscillation or angle-dependent magneto-resistance experiments exist. Insight into the average quasiparticle mass of overdoped LSCO stems, therefore, alone from specific heat measurements[34]. Compared to Tl2201[15], a somewhat larger Sommerfeld constant $\gamma_{el} \simeq 12$ mJ/(mole K^2) is found for overdoped LSCO $x \simeq 0.23$[34], suggesting a larger average quasiparticle mass. This is not necessarily inconsistent with the ARPES data. The Fermi-liquid cut-off energy scale, ω_c, softens rapidly as a function of Fermi surface angle, and the quasiparticle scattering is globally dependent on momentum[20]. This implies (1) that the contribution from non-Fermi liquid excitations will become increasingly important and (2) that $\hat{Z} < 1$ on certain portions of the Fermi surface. Both effects would lead to larger quasiparticle masses.

V. CONCLUSIONS

In summary, we have proven that the nodal single particle excitations observed by ARPES in overdoped LSCO are indeed true Landau Fermi liquid quasiparticle excitations. This result, together with consistent MDC and EDC analysis, was obtained without knowing the exact bare band. From Kramers-Kronig consistency of the quasiparticle self-energy Σ, insight into the bare band ϵ_b and the real part of the self-energy Σ' were obtained. An estimate of the nodal quasiparticle residue $Z = 0.42(7)$ allowed comparison to quasiparticle masses obtained from thermodynamic and high-field quantum oscillation experiments on overdoped $Tl_2Ba_2CuO_{6+\delta}$ compounds[6].

Acknowledgments: This work was supported by the Swiss NSF (through NCCR, MaNEP, and grant Nos. 200020-105151 and PZ00P2-142434), the Ministry of Education and Science of Japan, and the Swedish Research Council. The experimental work was performed at the SLS of the Paul Scherrer Institut, Villigen PSI, Switzerland. We thank the X09LA beamline[19] staff for their technical support.

[1] D. Pines and P. Nozieres, *The theory of quantum liquids* (W. A. Benjamin, 1966).
[2] S. I. Mirzaei, D. Stricker, J. N. Hancock, C. Berthod, A. Georges, E. van Heumen, M. K. Chan, X. Zhao, Y. Li, M. Greven, et al., PNAS **110**, 5774 (2013).
[3] N. Barišić, M. K. Chan, Y. Li, G. Yu, X. Zhao, M. Dressel, A. Smontara, and M. Greven, PNAS **110**, 12235 (2013).
[4] S. Nakamae, K. Behnia, N. Mangkorntong, M. Nohara, H. Takagi, S. J. C. Yates, and N. E. Hussey, Phys. Rev. B **68**, 100502 (2003).
[5] N. Doiron-Leyraud, C. Proust, D. LeBoeuf, J. Levallois, J.-B. Bonnemaison, R. Liang, D. A. Bonn, W. N. Hardy, and L. Taillefer, Nature **447**, 565 (2007).
[6] B. Vignolle, A. Carrington, R. A. Cooper, M. M. J. French,

A. P. Mackenzie, C. Jaudet, D. Vignolles, C. Proust, and N. E. Hussey, Nature **455**, 952 (2008).
[7] S. E. Sebastian, N. Harrison, and G. G. Lonzarich, Rep. Prog. Phys. **75**, 102501 (2012).
[8] B. Vignolle, D. Vignolles, D. LeBoeuf, S. Lepault, B. Ramshaw, R. Liang, D. A. Bonn, W. N. Hardy, N. Doiron-Leyraud, A. Carrington, et al., C. R. Physique **12**, 446 (2011).
[9] Neven Barišić, Sven Badoux, Mun K. Chan, Chelsey Dorow, Wojciech Tabis, Baptiste Vignolle, Guichuan Yu, Jérôme Béard, Xudong Zhao, Cyril Proust and Martin Greven, Nat. Phys. **9**, 761-764 (2013).
[10] A. Damascelli, Z. Hussain, and Z.-X. Shen, Rev. Mod. Phys. **75**, 473 (2003).
[11] Jacko, A. C., Fjœrestad, J. O., and Powell, B. J., A unified explanation of the Kadowaki-Woods ratio in strongly correlated metals. Nat. Phys. **5**, 422-425 (2009).
[12] Jernej Mravlje, Markus Aichhorn, Takashi Miyake, Kristjan Haule, Gabriel Kotliar and Antoine Georges, Phys. Rev. Lett. **106**, 096401 (2011).
[13] Xiaoyu Deng, Jernej Mravlje, Rok Žitko, Michel Ferrero, Gabriel Kotliar and Antoine Georges, Phys. Rev. Lett. **110**, 086401 (2013).
[14] A. A. Kordyuk, S. V. Borisenko, A. Koitzsch, J. Fink, M. Knupfer, and H. Berger, Phys. Rev. B **71**, 214513 (2005).
[15] J. Loram, K. Mirza, J. Wade, J. Cooper, and W. Liang, Physica C: Superconductivity **235240, Part 1**, 134 (1994).
[16] M. Abdel-Jawad, M. Kennett, L. Balicas, A. Carrington, A. Mackenzie, R. H. McKenzie, and N. Hussey, Nat. Phys. **2**, 821 (2006).
[17] P. M. C. Rourke, A. F. Bangura, T. M. Benseman, M. Matusiak, J. R. Cooper, A. Carrington, and N. E. Hussey, New Journal of Physics **12**, 105009 (2010).
[18] There are at least two ways to mimic the effect of instrumental resolution. One is to use the measured Γ_0 and the width of the Fermi step that already include instrumental resolution. Another method is to use $\Gamma_0(intrinsic) = (\Gamma_0^2 - \Gamma_k(res)^2)^{0.5}$, where $\Gamma_k(res)$ is the momentum resolution, a Fermi step defined by k_BT and then convolve this with the instrumental resolution. Both methods where tried with essentially identical results.
[19] L. P. U. Flechsig and T. Schmidt, AIP Conf. Proc. **705**, 316 (2004).
[20] J. Chang, M. Månsson, S. Pailhés, T. Claesson, O. J. Lipscombe, S. M. Hayden, L. Patthey, O. Tjernberg, and J. Mesot, Nat. Comm. **4**, 2559 (2013).
[21] M. Månsson, T. Claesson, U. O. Karlsson, O. Tjernberg, S. Pailhés, J. Chang, J. Mesot, M. Shi, L. Patthey, N. Momono, et al., Rev. Sci. Instrum. **78**, 076103 (2007).
[22] O. Lispcompe, S. M. Hayden, B. Vignolle, D. F. McMorrow and T. G. Perring, Phys. Rev. Lett. **99**, 067002 (2007)
[23] Chang, J., *et al.*, Phys. Rev. B **85**, 134520 (2012).
[24] X. J. Zhou, T. Yoshida, A. Lanzara, P. V. Bogdanov, S. A. Kellar, K. M. Shen, W. L. Yang, F. Ronning, T. Sasagawa, T. Kakeshita, et al., Nature **423**, 398 (2003).
[25] T. Yoshida, X. J. Zhou, D. H. Lu, S. Komiya, Y. Ando, H. Eisaki, T. Kakeshita, S. Uchida, Z. Hussain, Z.-X. Shen, et al., J. Phys.: Cond. Matt. **19**, 125209 (2007).
[26] J. Chang, M. Shi, S. Pailhés, M. Månsson, T. Claesson, O. Tjernberg, A. Bendounan, Y. Sassa, L. Patthey, N. Momono, et al., Phys. Rev. B **78**, 205103 (2008).
[27] E. Abrahams and C. M. Varma, PNAS **97**, 5714 (2000).
[28] G.-H. Gweon, B. S. Shastry, and G. D. Gu, Phys. Rev. Lett. **107**, 056404 (2011).
[29] E. Pavarini, I. Dasgupta, T. Saha-Dasgupta, O. Jepsen, and O. K. Andersen, Phys. Rev. Lett. **87**, 047003 (2001).
[30] J. Geck et al., Phys. Rev. Lett. **99**, 046403 (2007)
[31] C. Varma, Z. Nussinov, and W. van Saarloos, Physics Reports **361**, 267 (2002).
[32] J. Kokalj and R. H. McKenzie, Phys. Rev. Lett. **107**, 147001 (2011).
[33] J. Kokalj, N. E. Hussey, and R. H. McKenzie, Phys. Rev. B **86**, 045132 (2012).
[34] N. Momono, M. Ido, T. Nakano, M. Oda, Y. Okajima, and K. Yamaya, Physica C: Superconductivity **233**, 395 (1994).